DOI: 10.6060/ivkkt.20226510.6596

УДК: 544.016+544.77

СРАВНИТЕЛЬНЫЙ АНАЛИЗ ТЕРМИЧЕСКИХ И МЕХАНИЧЕСКИХ СВОЙСТВ ПОЛИМЕРНЫХ КОМПОЗИТОВ, АРМИРОВАННЫХ НАНОЦЕЛЛЮЛОЗОЙ, ПОЛУЧЕННОЙ СЕРНОКИСЛОТНЫМ ГИДРОЛИЗОМ И ТЕМПО-ОКИСЛЕНИЕМ

М.И. Воронова, О.В. Суров, М.М. Кузиева, А.А. Атаханов

Марина Игоревна Воронова (ORCID 0000-0002-8535-6940), Олег Валентинович Суров (ORCID 0000-0002-7164-364X)*

Лаборатория физической химии гетерогенных систем полимер-жидкость, Институт химии растворов им. Г.А. Крестова РАН, ул. Академическая, 1, Иваново, Российская Федерация, 153045
E-mails: miv@isc-ras.ru, ovs@isc-ras.ru*

Махлиё Мухаммадиевна Кузиева (ORCID 0000-0003-2552-6941), Абдумутолиб Абдупаттаевич Атаханов (ORCID 0000-0002-4975-3658)

Лаборатория физических и физико-химических методов исследования, Институт химии и физики полимеров, Академия наук Республики Узбекистан, ул. Кадырий, 76, Ташкент, Республика Узбекистан, 100128
E-mails: makhliyokuziyeva92@gmail.com, a-atakhanov@yandex.ru

Основным недостатком нанокристаллической целлюлозы (НКЦ), полученной традиционным сернокислотным гидролизом, является ее низкая термическая стабильность вследствие пиролиза, катализируемого поверхностными сульфогруппами. Замена поверхностных сульфогрупп карбоксильными (в результате окисления) позволяет значительно повысить термическую стабильность НКЦ. Несмотря на большое количество публикаций, описывающих свойства полимерных нанокомпозитов, армированных НКЦ, термическая устойчивость таких композитов до сих пор плохо изучена, а литературные данные часто противоречивы. В данной работе НКЦ получали из микрокристаллической целлюлозы двумя способами: сернокислотным гидролизом и окислением (2,2,6,6-тетраметилпиперидин-1-ил)оксилом (ТЕМПО). Получены композиты НКЦ с водорастворимыми полимерами – поливиниловым спиртом, полиэтиленоксидом, поливинилпирролидоном и полиакриламидом. Композиты были охарактеризованы различными методами, а именно: просвечивающей электронной и растровой электронной микроскопией, энергодисперсионным рентгеноспектральным анализом, инфракрасной Фурье-спектроскопией, рентгеноструктурным и термогравиметрическим анализами, дифференциальной сканирующей калориметрией, испытаниями на растяжение. Проведено сравнительное изучение термических и механических свойств полимерных композитов, армированных наноцеллюлозой, полученной сернокислотным гидролизом и ТЕМПО-окислением. Анализ термических свойств НКЦ показывает, что замена поверхностных сульфогрупп на карбоксильные приводит к значительному повышению температуры начала термического разложения и температуры максимальной скорости разложения НКЦ. Однако термическое поведение композитов с полимерами намного сложнее, что подробно обсуждается в представленном материале. Анализ механических свойств композитов показал, что добавление наноцеллюлозы, полученной ТЕМПО-окислением, не приводит к существенному улучшению прочности на разрыв и модуля Юнга по сравнению с наноцеллюлозой, полученной сернокислотным гидролизом.

Ключевые слова: нанокристаллы целлюлозы, сернокислотный гидролиз, ТЕМПО-окисление, полимерные композиты, термические и механические свойства

Для цитирования:
Воронова М.И., Суров О.В., Кузиева М.М., Атаханов А.А. Сравнительный анализ термических и механических свойств полимерных композитов, армированных наноцеллюлозой, полученной сернокислотным гидролизом и ТЕМПО-окислением. *Изв. вузов. Химия и хим. технология*. 2022. Т. 65. Вып. 10. С. 95–105. DOI: 10.6060/ivkkt.20226510.6596.

For citation:
Voronova M.I., Surov O.V., Kuziyeva M.K., Atakhanov A.A. Thermal and mechanical properties of polymer composites reinforced by sulfuric acid-hydrolyzed and TEMPO-oxidized nanocellulose: a comparative study. *ChemChemTech* [*Izv. Vyssh. Uchebn. Zaved. Khim. Khim. Tekhnol*.]. 2022. V. 65. N 10. P. 95–105. DOI: 10.6060/ivkkt.20226510.6596.

THERMAL AND MECHANICAL PROPERTIES OF POLYMER COMPOSITES REINFORCED BY SULFURIC ACID-HYDROLYZED AND TEMPO-OXIDIZED NANOCELLULOSE: A COMPARATIVE STUDY

M.I. Voronova, O.V. Surov, M.K. Kuziyeva, A.A. Atakhanov

Marina I. Voronova (ORCID 0000-0002-8535-6940), Oleg V. Surov (ORCID 0000-0002-7164-364X)*

Laboratory of Physical Chemistry of Polymer-Liquid Heterogeneous Systems, G.A. Krestov Institute of Solution Chemistry of the RAS, Akademicheskaya st., 1, Ivanovo 153045, Russia
E-mails: miv@isc-ras.ru; ovs@isc-ras.ru*

Makhliyo M. Kuziyeva (ORCID 0000-0003-2552-6941), Abdumutolib A. Atakhanov (ORCID 0000-0002-4975-3658)

Laboratory of Physical and Physicochemical Methods of Investigations, Institute of Polymer Chemistry and Physics, Academy of Sciences of Republic of Uzbekistan, Kadiriy st., 7b, Tashkent 100128, Republic of Uzbekistan
E-mails: makhliyokuziyeva92@gmail.com; a-atakhanov@yandex.ru

The main drawback of cellulose nanocrystals (CNCs) obtained by conventional sulphuric acid hydrolysis is their low thermal stability in consequence of pyrolysis catalyzed by sulfo-groups on the CNC surface. Replacement of surface sulfo-groups by carboxyl groups as a result of oxidation allows the thermal stability of CNCs to be enhanced significantly. Although a great number of studies have reported properties of polymer nanocomposites reinforced by CNCs, thermal properties of the composites compared to the neat polymers are discrepant and still poorly understood. In this work, CNCs were produced from microcrystalline cellulose by sulfuric acid hydrolysis and (2,2,6,6-tetramethylpiperidin-1-yl)oxyl (TEMPO) oxidation. The CNC composites with water-soluble polymers – polyvinyl alcohol, polyethylene oxide, polyvinylpyrrolidone and polyacrylamide – were obtained. The composites were characterized by various methods, i.e. transmission electron and scanning electron microscopies, energy-dispersive X-ray analysis, Fourier-transform infrared spectroscopy, X-ray diffraction and thermogravimetric analyses, differential scanning calorimetry, and tensile testing. A side-by-side comparison between the thermal and mechanical properties of the polymer composites reinforced by sulfuric acid-hydrolyzed and TEMPO-oxidized nanocellulose was conducted. Analysis of the thermal properties of CNC shows that the surface sulfonate groups replacement with carboxyl groups leads to significant increase of initial temperature of thermal degradation and temperature of the maximum decomposition rate of the CNC. However, the thermal behavior of the composites is much more complicated, and such thermal properties are discussed in detailed. The tensile properties analysis of the composites demonstrates that an addition of TEMPO-oxidized nanocellulose does not improve significantly the tensile strength and Young's modulus as compared with sulfuric acid-hydrolyzed one.

Key words: cellulose nanocrystals, sulfuric acid hydrolysis, TEMPO oxidation, polymer composites, thermal and mechanical properties

INTRODUCTION

Cellulose is one of most available renewable natural resources with annual production rate more than 90 billion tons. As a cheap biopolymer cellulose plays an important role in production of ecologically pure biocompatible and biodegradable functional materials. Rod-like particles of cellulose nanocrystals (CNCs) can be isolated from cellulose fibers under acid or enzymatic hydrolysis conditions. Dimension of these particles ranges from 100 to 1000 nm in length and from 5 to 50 nm in diameter depending on hydrolysis conditions and raw material used [1, 2].

At present, CNCs attract attention by material scientists not only due to their availability and ecological compatibility but also because of unique combination of physical and chemical properties: low toxicity and biocompatibility, biodegradability, large specific surface area and high modulus of elasticity [3, 4]. The application of CNCs as fillers in polymers allows materials to gain new quality improving their mechanical, optical and sorption properties, electrical performance, and control humidity.

The application of biodegradable polymers and polymeric composite materials attracts increasing attention due to environmental protection issues arose. Nowadays, a tendency to use natural organic nanofillers is caused by their advantages compared to conventional inorganic fillers: biodegradability and low toxicity. The use of CNCs as nano-dimentional elements for reinforcement of polymeric matrices is of interest due to unique combination of required physical and chemical properties and environmental benefits [5-10].

The main drawback of the CNCs obtained by conventional sulphuric acid hydrolysis is low thermal stability of the CNCs (owing to pyrolysis that is catalyzed by sulfo-groups on their surface) [11]. However, replacement of sulfuric acid with other mineral or organic acids usually brings to a limited dispersive ability of CNCs in polar media and increases flocculation of their aqueous suspensions due to insufficient surface charge of the CNC particles. Therefore, in this case a combination of hydrolysis and preceding or succeeding oxidation of cellulose is often applied [12, 13]. Frequently for cellulose oxidation, (2,2,6,6-tetramethylpiperidin-1-yl)oxyl (TEMPO) is used, which oxidizes primary hydroxyl groups of the cellulose to carboxyl groups. Other oxidizers are also applied, e.g., hydrogen peroxide, ammonium persulfate, $NaNO_2$-HNO_3, etc. [14-18]. The cellulose oxidation is accompanied with the formation of surface carboxyl groups which favor a good dispersive ability of CNCs in polar media as well as in polymer matrices of the composites. Introduction of carboxyl groups into CNCs may increase their interphase interaction with a hydrophobic polymer matrix because of enhancement of the CNC dispersion stability in different organic solvents which are good to solve the polymer. Carboxyl groups participate in covalent cross-linking and grafting reactions, they bring to adsorption of small molecules and ions as well as make them highly effective sites for inorganic functional nanoparticles fixing [19]. It is a very important circumstance that, in contrast to the surface sulfo-groups, carboxyl groups do not reduce the thermal stability of CNCs [20].

In this work, to obtain composites, the following water-soluble polymers were used: polyvinyl alcohol (PVA), polyethylene oxide (PEO), polyvinylpyrrolidone (PVP), and polyacrylamide (PAM).

PVA and PEO are water-soluble synthetic semicrystalline polymers with numerous industrial and commercial applications due to their biodegradability, biocompatibility, chemical resistance and excellent physical properties [21, 22].

PVP and PAM are water-soluble non-ionogenic amphoteric polymers. PVP is characterised by high solubility in water and polar solvents and is broadly used in synthesis of nanoparticles [23]. PVP, due to its amphiphilic nature, may affect the morphology and shape of the nanoparticles governing the growth of certain crystal faces [24-26]. PAM is used as a selective flocculant in purification of domestic and industrial wastewaters, trapping and extraction heavy metal ions and toxic compounds in mining, ore beneficiation and regeneration of valuable mineral deposits (uranium, gold, titanium, aluminium, iron and charcoal) [27]. Addition of PAM as a binder to paper pulp increases fillers and pigments retention within the pulp in a wet and dry state. In oil industry, it is used as a stabilizer in drilling, for control of a filterability and rheological properties of drilling fluids.

A great number of studies have reported properties of polymer nanocomposites reinforced by CNCs [28-33]. Although most of the CNC-based polymer composites have shown a significant improvement in mechanical and barrier properties, their thermal properties compared to the neat polymers are discrepant and still poorly understood. Inconsistencies in the results published may be explained by different characteristics of polymers used for composite preparation. The starting polymer can vary greatly in properties (molecular weight, degree of hydrolysis, degree of crystallinity, etc). Furthermore, thermal behavior of the composites depends also on CNC properties, i.e., the origin, preparation conditions, distribution homogeneity in polymer matrix, etc. To the best of our knowledge, no attempts have been made in the literature to conduct a side-by-side comparison between thermal and mechanical properties of polymer composites reinforced by sulfuric acid-hydrolyzed and TEMPO-oxidized nanocellulose.

In this work, we present results on the effect of sulfuric acid-hydrolyzed and TEMPO-oxidized nanocellulose on mechanical and thermal properties of water-soluble polymer composites.

EXPERIMENTAL

Materials and methods

PVA, $(C_2H_4O)_n$, for synthesis (Mw approx. 30,000, degree of hydrolysis ≥98%) was purchased from Merck (Darmstadt, Germany). PEO, $(C_{2n}H_{4n+2}O_{n+1})$, for synthesis (Mw approx. 200,000) and PVP, $(C_6H_9NO)_n$, (average Mw 40,000) were purchased from Sigma-Aldrich (Saint Louis, MO, USA). PAM, $(C_3H_5NO)_n$, (average Mw 150,000) was purchased from Sigma-Aldrich (Moscow, Russia).

Microcrystalline cellulose (MCC) (~20 μm, powder, CAS No 9004-34-6, cotton linters) and (2,2,6,6-tetramethylpiperidin-1-yl)oxyl (TEMPO, $C_9H_{18}NO$, 98%, Mw 156.25) were purchased from Sigma-Aldrich (Saint Louis, MO, USA). Sodium hypochlorite (NaClO, 10-15%, reagent grade) was purchased from Acros Organics (New Jersey, USA). Sulfuric acid (H_2SO_4, chemically pure grade, GOST (State Standard) 4204-77) and sodium bromide (NaBr, chemically pure grade) were purchased from Chimmed (Moscow, Russia). Potassium bromide (KBr, FTIR grade, >99%), sodium hydroxide (NaOH, chemically pure grade) were purchased from Sigma-Aldrich (Moscow, Russia). Deionized water was used throughout the experiment.

Preparation of CNCs

Aqueous suspensions of CNCs were prepared by sulphuric acid hydrolysis of microcrystalline cellulose (MCC) according to procedure described earlier in [34]. Hydrolysis of MCC was conducted in water solution of sulphuric acid (62%, 1 g of MCC per 40 mL of solution) at 50 °C for 2 h with intensive stirring. The suspension obtained by hydrolysis was washed out from the acid with distilled water through multiple cycles repetition of centrifugation until the constant value of pH (~2.4) of the supernatant liquor was achieved. Further, the CNC suspension was purified with ion-exchange resin (TOKEM MB-50(R), Germany) and dialysis (cutoff of 14 kDa, Roth, Germany), then sonicated (Sonorex DT100, Bandelin, Germany) for 15-30 min and used for preparation of polymer/CNC composite films. The CNC concentration in the suspensions was determined by gravimetry.

For the TEMPO-oxidized CNC preparation, the CNCs were used preliminary treated with sodium hydroxide at elevated temperature for neutralization and surface sulfo-groups removal, as described in [19]. It was added 0.016 g of TEMPO and 0.1 g of sodium bromide to 2 mL of water and agitated in a magnetic stirrer for 60 min until complete dissolution attained [35]. Further water suspension of desulfated CNCs was added while stirring; the pH was adjusted to 10.0 ± 0.2 by 0.5 M NaOH addition and maintained this value during the whole procedure. Then 2.4 mL of NaClO solution was added drop by drop with constant stirring. After completion of the oxidation reaction, approximately in 1 h, the pH was adjusted to 7, and 30 mL of ethanol was added to the suspension to avoid further oxidation.

The CNC samples obtained by conventional sulphuric acid hydrolysis are denoted below as SCNC, desulphated CNC samples as DCNC, and TEMPO-oxidized samples as TCNC.

Preparation of composites

For the composites preparation, 0.5 g of the polymer (PVA, PEO, PVP, or PAM) was dissolved in water (10 mL) at room temperature with constant stirring for two hours. Into the obtained polymer solution (5%), a required amount of aqueous suspension of SCNC or TCNC was added to prepare composites with different content of the SCNC or TCNC. The mixtures obtained were agitated vigorously for one more hour. The films of the composites were formed by pouring into glass Petri dishes and dried at room temperature for 24-48 h. The composite films with different content of SCNC or TCNC (5, 10, 20 etc. wt. %) were labeled as PAM/SCNC-5, PEO/TCNC-10 and so on.

Characterization

The size of CNC particles was determined by using a LEO 912 AB OMEGA transmission electron microscope (TEM) (Carl Zeiss, Germany) with energy filter integrated in the optical system of the instrument. The Köhler system provides even illumination of the sample with the parallel electron beam. The automated system allows illumination only of that sample area which is appeared on the fluorescent screen of the microscope to prevent unwanted electron beam damage of other parts of the sample. The main features of the microscope are as follows: accelerating voltage (60, 80, 100, 120 kV), irradiated region (1-75 μm), aperture (0.2-0.34 mrad), magnification (from 80x to 500 000x), inelastic scattering resolution (1.5 eV), energy range of inelastic scattering measurement (0-2500 eV).

A NanoAnalysis energy-dispersive X-ray spectrometer (Oxford Instruments, UK) with an 'x-ACT' detector synchronized with a electron gun of a VEGA 3 SBH TESCAN (Czech Republic) scanning electron microscope (SEM) was used for elemental analysis of the sample surfaces.

The CNC particles size and charge in aqueous suspensions were determined by dynamic light scattering (DLS) method with a Zetasizer Nano ZS (Malvern Instruments Ltd, UK) analyzer.

The FTIR spectra were obtained using a VERTEX 80v spectrophotometer (Bruker, Germany) in the frequency range of 4000-400 cm^{-1}. The samples were pressed in pellets containing 1 mg of the compound to be analyzed and 100 mg of potassium bromide.

For the thermogravimetric analysis, a TG 209 F1 Iris thermomicrobalance (Netzsch, Germany) with platinum crucibles in a dry argon atmosphere at a flow rate of 30 mL min^{-1}, and a heating rate of 10 K min^{-1}, was used.

The thermal properties of the composites were studied using a DSC 204 F1 'Phoenix' (Netzsch, Germany) differential scanning heat flux calorimeter (DSC). The calorimetric experiment was conducted in a dry argon atmosphere (ultra high purity grade, 99.998% argon content) at a flow rate of 15 mL min^{-1} and a heating rate of 10 K min^{-1} using standard aluminum crucibles.

The degree of polymer crystallinity in the CNC composite can be calculated by the equation:

$$\chi_c = \Delta H_m / w\, \Delta H^0_m, \quad (1)$$

where w is the mass fraction of the polymer in the composite; ΔH_m is the heat of fusion of the composite measured from DSC thermograms, and ΔH^0_m is the heat of fusion of the 100% crystalline neat polymer.

The elemental analysis was performed with a Flash EA-1112 (Thermo Quest, Italy) analyzer and a NanoAnalysis energy-dispersive X-ray spectrometer (Oxford Instruments, UK).

The X-ray diffraction analysis was conducted with a Bruker D8 Advance powder diffractometer (Bruker, Germany) according to the Bragg-Brentano geometry using Cu-K_α radiation (λ = 0.1542 nm). The angular scanning range was 2-45° with 0.01° step. A Vantec-1 count rate detector was used. The impulses counting time at each scanning point was 0.5 s. The crystallinity index was calculated according to the Segal method [5]:

$$IC = (I_{200} - I_a)/I_{200}, \quad (2)$$

where I_{200} is the reflex intensity corresponding to the crystallographic plane (200), I_a is an amorphous halo intensity - minimum between the two peaks, corresponding to the crystallographic planes (200) and (110).

The crystallite sizes L (nm) (CNCs or a crystalline polymer) were calculated using the Scherrer equation [37]:

$$L = 0.9\,\lambda / \beta\, \mathrm{Cos}\, \Theta, \quad (3)$$

where λ is the wavelength of X-ray radiation (nm); β is the full width at half height of the diffraction peak (rad); Θ is the reflex angle (deg).

The tensile properties of the composite films were measured using an I 1158 M-2.5-01-1 tension testing machine (Russia) in the tension mode at room temperature at the maximum load of 5 kN and minimum loading rate of 1 mm min^{-1}. Five specimens with the dimensions of 15 mm (length)×5 mm (width)×0.1 mm (thickness) were used for each sample group. The stress and strain values were calculated from the machine-recorded force and displacement based on the initial cross-section area and the original gauge length (10 mm) of each sample, respectively. The Young's modulus for each sample was calculated from the initial linear portion of the stress-strain curves through a linear regression analysis. The obtained values of the Young's modulus were within ±10%, while the stress and the elongation at break fluctuated in the range of ±15%. The thickness of the samples was estimated throughout the sample surface using a RECXON GY-910 thickness gauge (China) with a combined measurement principle (electromagnetic induction, Foucault eddy currents) with a measurement range of 0–1300 μm and a measurement accuracy of 3%. The resulting composite films were about 100 μm thick.

RESULTS AND DISCUSSION

The images of SCNC and TCNC particles obtained with a transmission electron microscope (TEM) are shown in Fig. 1.

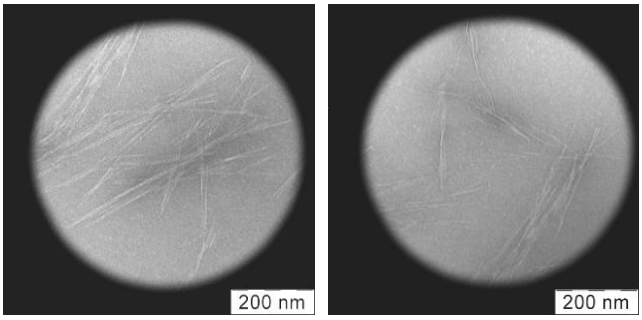

a b

Fig. 1. TEM images of SCNC (a) and TCNC (b) particles. The scale is 200 nm

Рис. 1. Изображения частиц SHKЦ (a) и THKЦ (b), полученные с помощью просвечивающего электронного микроскопа. Масштаб: 200 нм

The X-ray diffraction patterns of the SCNC and TCNC samples are shown in Fig. 2. The diffraction peak arising at ~ 2θ = 22.9° is assigned to the (200) plane of cellulose $I_ß$, and the two overlapped weaker diffractions at 2θ close to 16.6 and 14.8° are attributed to the (110) and (1-10) lattice planes of cellulose $I_ß$ [36].

Physicochemical characteristics of the SCNC and TCNC samples along with the methods and equipment used are presented in Table 1.

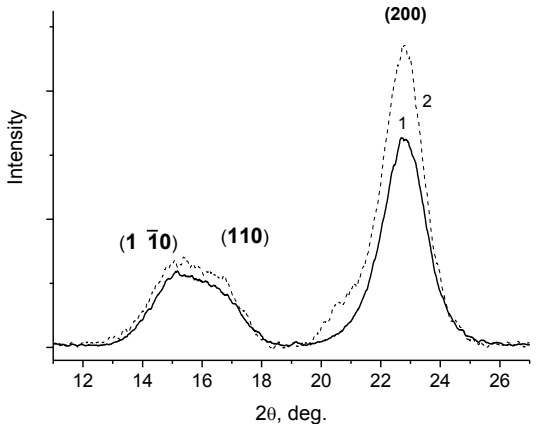

Fig. 2. X-ray diffraction patterns of the SCNC (1) and TCNC (2) samples
Рис. 2. Рентгеновские дифрактограммы образцов SHКЦ (1) and THКЦ (2)

Table 1

Characteristics of the SCNC and TCNC samples
***Таблица 1.* Характеристики образцов SHКЦ and THКЦ**

Parameter	Characteristics	
	SCNC	TCNC
[a] Dimensions of the particles, nm		
length	200-400	200-400
diameter	10-20	10-20
[b] Hydrodynamic diameter, nm	310±20	300±30
[b] ζ-potential, mV	-40	-30
[c] Total sulfer content, %	0.9	-
[d] Degree of polymerization	80	80
[e] Crystallinity index, %	83.8	83.0
[e] Crystallite size in (200) plane, nm	4.1	4.1

Notes: [a]Transmition electron microscopy (LEO 912 AB OMEGA)
[b]Dynamic light scattering (Zetasizer Nano-ZS)
[c]Elemental analysis (Flash EA-1112)
[d]Determined through viscosity measurements of CNC solutions in cadoxene
[e]X-ray diffraction analysis (Bruker D8 Advance)
Примечания: [a]Просвечивающая электронная микроскопия (LEO 912 AB OMEGA)
[b]Динамическое рассеивание света (Zetasizer Nano-ZS)
[c]Элементный анализ (Flash EA-1112)
[d]Рассчитано на основе данных по измерению вязкости растворов НКЦ в кадоксене
[e]Рентгеновский дифракционный анализ (Bruker D8 Advance)

Table 2

Elemental composition of the CNC samples according to X-ray energy dispersive analysis
***Таблица 2.* Элементный состав образцов НКЦ по данным рентгеновского энерго-дисперсионного анализа**

Sample	Elemental composition, %			
	C	O	S	Na
SCNC	51.3	46.8	0.9	0.7
DCNC	49.1	48.9	0.4	0.3
TCNC	52.2	47.8	-	0.4

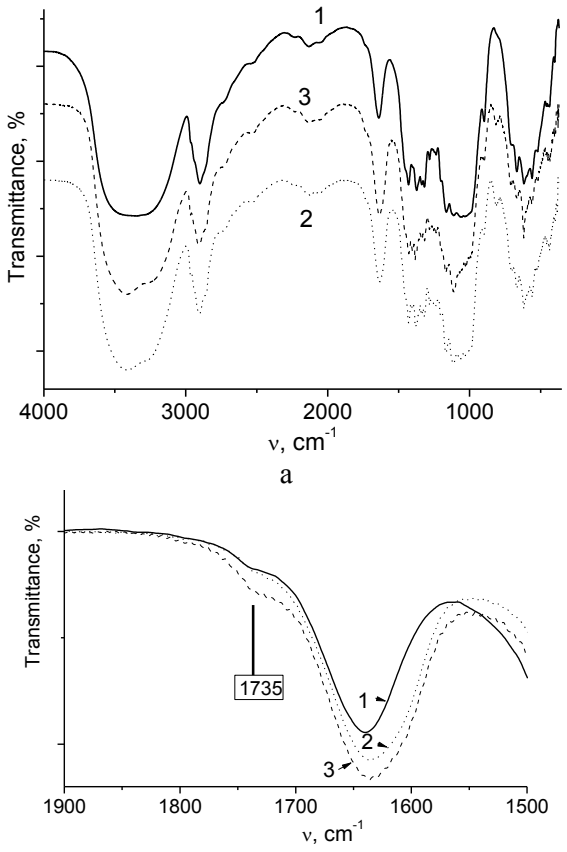

Fig. 3. The FTIR spectra of the SCNC (1), DCNC (2) and TCNC (3) samples in the range of wavenumbers 4000-400 cm^{-1} (a), and in the range of wavenumbers 1900-1500 cm^{-1} (b)
Рис. 3. ИК спектры образцов SHКЦ (1), DHКЦ (2) и THКЦ (3) в диапазоне волновых чисел 4000-400 $см^{-1}$ (a) и 1900-1500 $см^{-1}$ (b)

The results of elemental analysis (Table 2) indicate that desulfation of CNCs helps to reduce amount of surface sulfo-groups considerably. The surface sulfo-groups are removed completely through the TEMPO-oxidation procedure and surface carboxyl groups are formed that is clearly seen from the FTIR spectra (Fig. 3) of the TCNC samples (the C=O valence vibrations band at 1735 cm^{-1}).

Thermal stability is a very important characteristic that should be considered in uses of nanocomposites in various industrial fields. The study of degradation behavior is necessary for designing polymer composites with required performance and enhanced thermal stability. As the decomposition temperature of CNCs is about 200 °C, polymer processing temperature must not exceed that value to prevent their degradation. Numerous factors, including methods of CNC isolation, the cellulose source, the crystallinity of CNCs, and the sulfate content have profound effects on their thermal stability. The high content of surface sulfo-groups after sulfuric acid hydrolysis can decrease the thermal stability of CNC-based polymer composites [37]. Moreover, the thermal stability of polymer composites depends strongly on the strength

of intermolecular bonding between CNCs and a polymer matrix [38]. Therefore, for the enhanced thermal stability of polymer composites, a good interfacial adhesion between CNCs and a polymer matrix is needed. Hence, improving the thermal stability of polymer composites with CNCs obtained by sulfuric acid hydrolysis, remains a great challenge.

Analysis of TG and DTG curves shows that replacement of surface sulfo-groups with carboxyl groups brings to a significant increase of initial degradation temperature and temperature of the maximum decomposition rate of the CNC samples studied (from 170 to 308 °C) (Fig. 4).

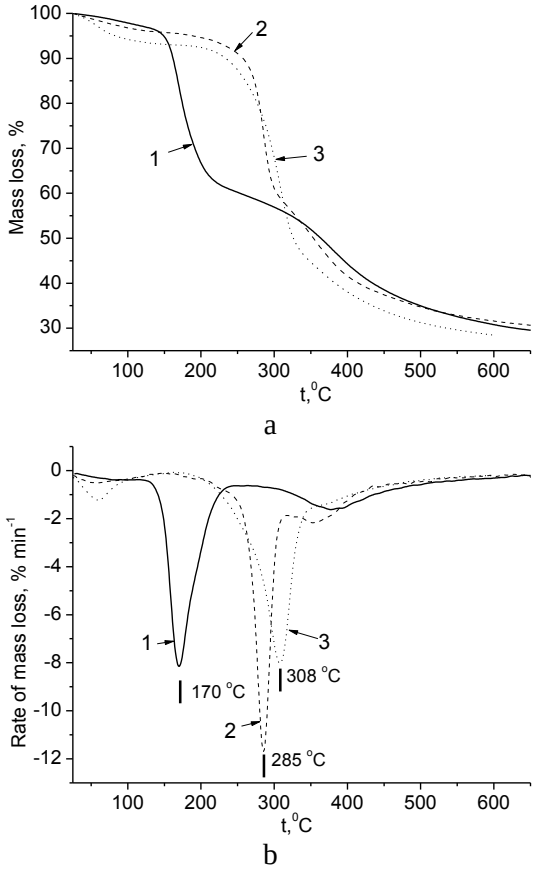

Fig. 4. TG (a) and DTG (b) curves for the SCNC (1), DCNC (2), and TCNC (3) samples
Рис. 4. ТГ (a) и ДТГ (b) кривые образцов SHKЦ (1), DHKЦ (2) и THKЦ (3)

However, the thermal stability and degradation behavior of polymer composites based on SCNC and TCNC samples are much more complicated. In the thermograms obtained, three main mass loss regions can be observed. All of the samples show an initial mass loss in the region 80-150 °C attributable to the evaporation of water. The second degradation region is located between 250 and 400 °C and is attributed to pyrolysis of CNC and to the degradation of a polymer. The second stage of degradation mainly involves dehydration reactions and the formation of volatile products. The third stage of mass loss occurs above 400 °C and involves the decomposition of carbonaceous matter [38]. Pyrolysis of CNC results in the increasing amount of char residue for polymer composites in comparison with the neat polymers.

The composites studied demonstrate common thermal behavior: with an increase of CNC content up to 30%, a low temperature peak appears due to thermal destruction of SCNC while TCNC in the composites decays at a higher temperature. The temperatures of thermal decomposition of SCNC and TCNC in PEO- and PVP-based composites are increased significantly and are about 250 and 350 °C for SCNC and TCNC, respectively [22, 23]. However, in PAM-based composite, practically no difference in decomposition behavior of SCNC and TCNC is observed [27].

The thermal stability of PVA-based composites differs remarkably compared to others in the series of studied polymers. As is seen in Fig. 5, the temperature of the maximum decomposition rate of the composite in the presence of TCNC or SCNC grows up to 330 °C or 380 °C, respectively, as compared with 290 °C for the neat PVA. Earlier we have shown that thermal degradation of both SCNC and PVA in the composite occurs simultaneously at a much higher temperature than that of the SCNC or the neat PVA, and thermal stability of the PVA-based composites is maximally enhanced with the SCNC content of 8-12 wt% [21]. The enhanced thermal stability of PVA/SCNC composites is related to three-dimensionally cross-linked structures formed from high-molecular-weight conjugated polyenes forming during the PVA thermal dehydration (in the presence of SCNC acting as dehydrating agent).

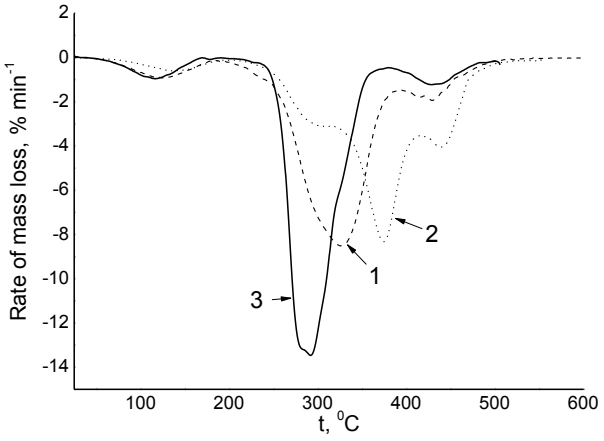

Fig. 5. DTG curves for PVA/TCNC-10 (1) and PVA/SCNC-10 (2) composites. For comparison, the curve for the neat PVA is shown (3)
Рис. 5. ДТГ кривые композитов ПВС/THKЦ-10 (1) и ПВС/SHKЦ-10 (2). Для сравнения показана также ДТГ кривая для чистого ПВС (3)

Thermal properties of polymer composites were determined using differential scanning calorimetry (DSC) as well. The DSC for composites based on PVA and PEO exhibit sharp enough endothermic peaks [21, 22], corresponding to the melting of the crystalline phase of PVA or PEO. The melting temperature (T_m), crystallization temperature (T_{cryst}), heat of fusion (ΔH_m), and degree of crystallinity (χ_c) obtained from the DSC data for semicrystalline polymers, PEO and PVA, are collected in Table 3.

Table 3

Melting temperature (T_m), crystallization temperature (T_{cryst}), heat of fusion (ΔH_m), and degree of crystallinity (χ_c) of PEO and PVA in composites with SCNC and TCNC

Таблица 3. **Температура плавления (T_m), температура кристаллизации (T_{cryst}), теплота плавления (ΔH_m) и степень кристалличности (χ_c) ПЭО и ПВС в композитах с SHКЦ и ТНКЦ**

Sample	T_m, °C	T_{cryst}, °C	ΔH_m, J g^{-1}	χ_c, %
PEO	65.5	36.3	138.2	73.5
PEO/SCNC-5	64.3	40.6	143.3	76.2
PEO/TCNC-5	68.1	36.0	136.2	68.8
PEO/SCNC-20	70.3	36.0	138.8	73.8
PEO/TCNC-20	64.6	39.4	101.0	67.1
PEO/SCNC-30	70.8	34.6	121.2	64.5
PEO/TCNC-30	64.7	37.6	93.2	70.8
PVA	227.9	192.4	78.4	48.7
PVA/SCNC-5	227.5	205.9	77.9	50.9
PVA/TCNC-5	223.8	207.0	73.3	47.9
PVA/SCNC-20	225.8	206.1	61.7	47.9
PVA/TCNC-20	223.7	191.6	61.9	47.9
PVA/SCNC-30	221.1	196.6	40.4	35.8
PVA/TCNC-30	222.3	185.7	47.2	41.9

The melting temperature and crystallization temperatures, heat of fusion, and degree of crystallinity have a complex behavior depending on CNC content in the composites, but tend to increase until the CNC content reached 5-10 wt.%, and decrease with further increasing the CNC content. That indicates that CNCs can act as nucleating agents and promote crystallization of polymer matrices at a lower CNC loading, and interrupt the regular packing of the polymer molecular chains at a higher CNC content [22]. The crystallinity of semicrystalline polymers is affected by nucleation and confinement caused by fillers [39]. Therefore, depending on the filler content in the composite, its crystallinity depends on the combined effects of nucleation and confinement. Moreover, poor dispersion and agglomeration of CNCs at their high concentration worsen the thermal stability of polymer composites based on CNCs.

However, the SCNC and TCNC based composites demonstrate apparently different behavior (Table 3). PVA and PEO are semicrystalline polymers bearing functional groups which produce strong molecular interactions (hydrogen bonding or van der Waals forces) between the polymers and SCNC or TCNC. A tighter packing and increased intermolecular bonding contribute to higher values of melting point, heat of fusion, and degree of crystallinity of the polymer composites. The differences in the surface functional groups of SCNC and TCNC affect the thermal behavior of their polymer composites.

The glass transition temperature (T_g) values for composites based on amorphous polymers (PVP and PAM) determined under heating and cooling are reported in Table 4.

Table 4

The glass transition temperature (T_g) of PVP and PAM in composites with SCNC and TCNC

Таблица 4. **Температура стеклования ПВП и ПАА в композитах с SHКЦ и ТНКЦ**

Sample	T_g, °C (heating)	T_g, °C (cooling)
PVP	180.2	166.7
PVP/SCNC-5	176.5	173.9
PVP/TCNC-5	163.1	161.0
PVP/SCNC-10	178.3	174.7
PVP/TCNC-10	162.3	162.0
PVP/SCNC-20	184.2	177.7
PVP/TCNC-20	162.9	162.8
PVP/SCNC-30	198.5	186.4
PVP/TCNC-30	165.9	163.3
PAM	194.5	193.3
PAM/SCNC-5	185.4	184.2
PAM/TCNC-5	179.7	186.6
PAM/SCNC-10	183.1	185.9
PAM/TCNC-10	184.7	183.6
PAM/SCNC-20	188.0	179.5
PAM/TCNC-20	191.3	193.2
PAM/SCNC-30	190.5	180.3
PAM/TCNC-30	187.9	182.6

The results of DSC analysis of PVP and PAM-based composites show that T_g values drop at CNC content of 5-10 wt.% initially and then tend to shift to higher T_g values with increasing the CNC content in the composite (Table 4). This higher T_g values can point out that the association of the polymer molecules is enhanced by the CNC presence. A noticeable increase in the T_g may be ascribed to the macromolecular confinement provided by SCNC or TCNC surfaces [40]. It is attributed to restrictions forced by intermolecular bonding between CNCs and the polymer matrices, which limit mobility and flexibility of the polymer chains and lead to an increase in the T_g. A strong hydrogen bonding between CNCs and the polymer matrices can lead to an increase in the T_g as

well. It is worth to note that the glass transition temperature of the PVP/TCNC composites is much lower than that of the PVP/SCNC. Apparently, this is due to the firmly bound water, which is not completely removed from the PVP/TCNC composites even under heating. The strongly bound water can act as a plasticizer and increase mobility of the polymer chains (the T_g decreases) [23].

Analysis of stress-strain curves and estimated tensile properties (Table 5) of the composites shows that CNC addition leads to enhancement of the tensile strength and decreases elongation at break. The TCNC addition does not demonstrate significant improvement of tensile properties compared to those of SCNC.

Table 5

Tensile properties of the composite films under study
***Таблица 5.* Прочностные свойства исследуемых композитных пленок**

Sample	Tensile strength at break (σ_b), MPa	Ultimate tensile strength (σ_{max}), MPa	Elongation at break (ε_b), %	Young's modulus (E), MPa
PVA	24±3.5	24±3.5	394±59.1	69±6.9
PVA/SCNC-10	20±3.0	20±3.0	245±36.8	122±12.2
PVA/TCNC-10	17±2.5	17±2.5	258±38.7	159±15.9
PVA/SCNC-30	30±4.5	30±4.5	288±43.2	155±15.5
PVA/TCNC-30	28±4.2	28±4.2	327±49.1	142±14.2
PAM	32±4.8	46±6.9	12±1.8	1380±138
PAM/SCNC-10	37±5.6	52±7.8	11±1.7	1360±136
PAM/TCNC-10	42±6.3	57±8.6	10±1.5	1650±165
PAM/SCNC-30	47±7.1	57±8.6	11±1.7	1270±127
PAM/TCNC-30	52±7.8	66±9.9	9±1.4	1400±140
PVP	7±1.0	10±1.5	7.5±1.1	133±13.3
PVP/SCNC-10	13±2.0	19±2.9	7.3±1.1	444±44.4
PVP/TCNC-10	16±2.4	19±2.9	6.9±1.0	587±58.7
PVP/SCNC-30	44±6.6	44±6.6	2.5±0.4	1140±114
PVP/TCNC-30	39±5.9	39±5.9	3.1±0.5	1280±128
PEO	2.6±0.4	2.7±0.4	1.7±0.3	150±15
PEO/SCNC-10	15±2.2	16±2.4	2.7±0.4	930±93
PEO/TCNC-10	20±3.0	20±3.0	2.8±0.4	1050±105
PEO/SCNC-30	26±3.9	27±4.1	3.2±0.5	1190±119
PEO/TCNC-30	28±4.2	29±4.4	3.2±0.5	1780±178

CONCLUSIONS

In this work, thermal and mechanical properties of composites of water soluble polymers (PVA, PAM, PVP, and PEO) with CNC prepared by sulfuric acid hydrolysis (SCNC) and TEMPO-oxidized (TCNC) were studied. Analysis of TG and DTG curves shows that the surface sulfonate groups replacement with carboxyl groups leads to significant increase of initial temperature of thermal degradation and temperature of the maximum decomposition rate of CNC. However, the thermal behavior of the composites is much more complicated. So, in the case of PAM, practically there is no any difference observed in the thermal decomposition behavior between PAM/SCNC and PAM/TCNC composites. The thermal stability of the PVA-based composites remarkably differs from other polymers. A temperature of the maximum decomposition rate of the composite is increased up to 330 °C for the TCNC and 380 °C for SCNC at their content of 10%, compared to 290 °C for the neat PVA. This is due to increased thermal stability of high-molecular structures formed during the thermal destruction process of PVA in the presence of SCNC as a dehydrating agent.

In the melting or crystallization behavior of semicrystalline polymers (PVA and PEO) in the composites with SCNC or TCNC, significant differences were not noticed. It was observed that the glass transition temperature of the PVP/TCNC composite is much lower than that for the PVP/SCNC composite, and that may be attributed to plastifying effect of the water trapped in the composite with TCNC.

The tensile properties analysis of the composites demonstrate that TCNC addition does not improve significantly the tensile strength and Young's modulus as compared with SCNC.

ACKNOWLEDGMENTS

The authors would like to thank The Upper Volga Region Centre of Physicochemical Research (Ivanovo, Russia) and Center for Shared Use of Scientific Equipment of the ISUCT of Ivanovo State University of Chemistry and Technology (grant of Ministry of Science and Higher Education of Russia № 075-15-2021-671) for some measurements carried out using the centers' equipment.

The authors declare the absence a conflict of interest warranting disclosure in this article.

Авторы выражают благодарность Верхневолжскому центру физико-химических исследований (Иваново, Россия) и Центру коллективного пользования научной аппаратурой Ивановского государственного химико-технологического университета (грант Минобрнауки России № 075-15-2021-671) за некоторые измерения, проведенные на оборудовании центров.

Авторы заявляют об отсутствии конфликта интересов, требующего раскрытия в данной статье.

REFERENCES
ЛИТЕРАТУРА

1. **Moon R.J., Martini A., Nairn J., Simonsen J., Youngblood J.** Cellulose nanomaterials review: structure, properties and nanocomposites. *Chem. Soc. Rev.* 2011. V. 40. N 7. P. 3941–3994. DOI: 10.1039/C0CS00108B.
2. **Nagarajan K.J., Balaji A.N., Ramanujam N.R.** Isolation and characterization of cellulose nanocrystals from Saharan aloe vera cactus fibers. *Int. J. Polym. Anal. Ch.* 2020. V. 25. N 2. P. 51–64. DOI: 10.1080/1023666X.2018.1478366.
3. **Klemm D., Kramer F., Moritz S., Lindström T., Ankerfors M., Gray D., Dorris A.** Nanocelluloses: A New Family of Nature-Based Materials. *Angew. Chem. Int. Ed.* 2011. V. 50. N 24. P. 5438-5466. DOI: 10.1002/anie.201001273.
4. **Habibi Y., Lucia L.A., Rojas O.J.** Cellulose Nanocrystals: Chemistry, Self-Assembly, and Applications. *Chem. Rev.* 2010. V. 110. N 6. P. 3479-3500. DOI: 10.1021/cr900339w.
5. **Kargarzadeh H., Ahmad I., Thomas S., Dufresne A.** Handbook of Nanocellulose and Cellulose Nanocomposites. New York: Wiley-VCH Verlag GmbH & Co. 2017. 920 p. DOI: 10.1002/9783527689972.
6. **Zhu H., Luo W., Ciesielski P.N., Fang Z., Zhu J.Y., Henriksson G., Himmel M.E., Hu L.** Wood-Derived Materials for Green Electronics, Biological Devices, and Energy Applications. *Chem. Rev.* 2016. V. 116. N 16. P. 9305-9374. DOI: 10.1021/acs.chemrev.6b00225.
7. **Thomas B., Raj M.C., Athira K.B., Rubiyah M.H., Joy J., Moores A., Drisko G.L., Sanchez C.** Nanocellulose, a Versatile Green Platform: From Biosources to Materials and Their Applications. *Chem. Rev.* 2018. V. 118. N 24. P. 11575-11625. DOI: 10.1021/acs.chemrev.7b00627.
8. **Dhali K., Ghasemlou M., Daver F., Cass P., Adhikari B.** A review of nanocellulose as a new material towards environmental sustainability. *Sci. Total Environ.* 2021. V. 775. ID 145871. DOI: 10.1016/j.scitotenv.2021.145871.
9. **Amara C., El Mahdi A., Medimagh R., Khwaldia K.** Nanocellulose-based composites for packaging applications. *Curr. Opin. Green Sustain. Chem.* 2021. V. 31. ID 100512. DOI: 10.1016/j.cogsc.2021.100512.
10. **Reshmy R., Thomas D., Philip E., Paul S.A., Madhavan A., Sindhu R., Binod P., Pugazhendhi A., Sirohi R., Tarafdar A., Pandey A.** Potential of nanocellulose for wastewater treatment. *Chemosphere* 2021. V. 281. ID 130738. DOI: 10.1016/j.chemosphere.2021.130738.
11. **Lin N., Dufresne A.** Surface chemistry, morphological analysis and properties of cellulose nanocrystals with gradiented sulfation degrees. *Nanoscale*. 2014. V. 6. P. 5384-5393. DOI: 10.1039/C3NR06761K.
12. **Yu X., Tong S., Ge M., Wu L., Zuo J., Cao C., Song W.** Adsorption of heavy metal ions from aqueous solution by carboxylated cellulose nanocrystals. *J. Environ. Sci.* 2013. V. 25. N 5. P. 933–943. DOI: 10.1016/S1001-0742(12)60145-4.
13. **Yu, H.-Y., Zhang D.-Z., Lu F.-F., Yao J.** New Approach for Single-Step Extraction of Carboxylated Cellulose Nanocrystals for Their Use As Adsorbents and Focculants. *ACS Sustain. Chem. Eng.* 2016. V. 4. N 5. P. 2632–2643. DOI: 10.1021/acssuschemeng.6b00126.
14. **Zhang K., Sun P., Liu H., Shang S., Song J., Wang D.** Extraction and comparison of carboxylated cellulose nanocrystals from bleached sugarcane bagasse pulp using two different oxidation methods. *Carbohydr. Polym.* 2016. V. 138. P. 237–243. DOI: 10.1016/j.carbpol.2015.11.038.
15. **Cheng M., Qin Z.Y., Liu Y.N., Qin Y.F., Li T., Chen L., Zhu M.F.** Efficient extraction of carboxylated spherical cellulose nanocrystals with narrow distribution through hydrolysis of lyocell fibers by using ammonium persulfate as an oxidant. *J. Mater. Chem. A.* 2014. V. 2. P. 251–258. DOI: 10.1039/C3TA13653A.
16. **Kumar V., Yang T.** HNO_3/H_3PO_4–$NaNO_2$ mediated oxidation of cellulose—preparation and characterization of bioabsorbable oxidized celluloses in high yields and with different levels of oxidation. *Carbohydr. Polym.* 2002.V. 48. N 4. P. 403–412. DOI: 10.1016/S0144-8617(01)00290-9.
17. **Xu Y., Liu X., Liu X., Tan J., Zhu H.** Influence of HNO_3/H_3PO_4–$NaNO_2$ mediated oxidation on the structure and properties of cellulose fibers. *Carbohydr. Polym.* 2014. V. 111. P. 955–963. DOI: 10.1016/j.carbpol.2014.05.029.
18. **Leung A.C., Hrapovic S., Lam E., Liu Y., Male K.B., Mahmoud K.A., Luong J.H.** Characteristics and properties of carboxylated cellulose nanocrystals prepared from a novel one-step procedure. *Small*. 2011. V. 7. N 3. P. 302–305. DOI: 10.1002/smll.201001715.
19. **Eyley S., Thielemans W.** Surface modification of cellulose nanocrystals. *Nanoscale*. 2014. V. 6. P. 7764-7779. DOI: 10.1039/C4NR01756K.
20. **Rubleva N.V., Lebedeva E.O., Afineevskii A.V., Voronova M.I., Surov O.V., Zakharov A.G.** Production of cellulose nanocrystals by hydrolysis in mixture of hydrochloric and nitric acids. *ChemChemTech [Izv. Vyssh. Uchebn. Zaved. Khim. Khim. Tekhnol.]*. 2019. V. 62. N 12. P. 85-93. DOI: 10.6060/ivkkt.20196212.5984.
Рублева Н.В., Лебедева Е.О., Афинеевский А.В., Воронова М.И., Суров О.В., Захаров А.Г. Получение нанокристаллической целлюлозы гидролизом в смеси соляной и азотной кислот. *Изв. вузов. Химия и хим. технология.* 2019. Т. 62. Вып. 12. С. 85-93. DOI: 10.6060/ivkkt.20196212.5984.
21. **Voronova M.I., Surov O.V., Guseinov S.S., Barannikov V.P., Zakharov A.G.** Thermal stability of polyvinyl alcohol/nanocrystalline cellulose composites. *Carbohydr. Polym.* 2015. V. 130. P. 440–447. DOI: 10.1016/j.carbpol.2015.05.032.
22. **Surov O.V., Voronova M.I., Afineevskii A.V., Zakharov A.G.** Polyethylene oxide films reinforced by cellulose nanocrystals: Microstructure-properties relationship. *Carbohydr. Polym.* 2018. V. 181. P. 489–498. DOI: 10.1016/j.carbpol.2017.10.075.
23. **Voronova M., Rubleva N., Kochkina N., Afineevskii A., Zakharov A., Surov O.** Preparation and Characterization of Polyvinylpyrrolidone/Cellulose Nanocrystals Composites. *Nanomaterials-Basel*. 2018.V. 8. N 12. ID 1011. DOI: 10.3390/nano8121011.
24. **Kyrychenko A., Korsun O.M., Gubin I.I., Kovalenko S.M., Kalugin O.N.** Atomistic Simulations of Coating of Silver Nanoparticles with Poly(vinylpyrrolidone) Oligomers: Effect of Oligomer Chain Length. *J. Phys. Chem. C*. 2015. V. 119. N 14. P. 7888–7899. DOI: 10.1021/jp510369a.
25. **Al-Saidi W.A., Feng H., Fichthorn K.A.** Adsorption of Polyvinylpyrrolidone on Ag Surfaces: Insight into a Structure-Directing Agent. *Nano Lett.* 2012. V. 12. N 2. P. 997–1001. DOI: 10.1021/nl2041113.
26. **Nathanael A.J., Seo Y.H., Oh T.H.** PVP Assisted Synthesis of Hydroxyapatite Nanorods with Tunable Aspect Ratio and Bioactivity. *J. Nanomater*. 2015. Art. ID 621785. DOI: 10.1155/2015/621785.
27. **Voronova M.I., Surov O.V., Afineevskii A.V., Zakharov A.G.** Properties of polyacrylamide composites reinforced by cellulose nanocrystals. *Heliyon* 2020. V. 6. N 11. ID e05529. DOI: 10.1016/j.heliyon.2020.e05529.

28. **Julkapli N.M., Bagheri S.** Progress on nanocrystalline cellulose biocomposites. *React. Funct. Polym.* 2017. V. 112. P. 9-21. DOI: 10.1016/j.reactfunctpolym.2016.12.013.
29. **Kontturi E., Laaksonen P., Linder M.B., Nonappa, Gröschel A.H., Rojas O.J., Ikkala O.** Advanced Materials through Assembly of Nanocelluloses. *Adv. Mater.* 2018. V. 30. N 24. ID 1703779. DOI: 10.1002/adma.201703779.
30. **Trache D., Tarchoun A.F., Derradji M., Hamidon T.S., Masruchin N., Brosse N., Hussin M.H.** Nanocellulose: From Fundamentals to Advanced Applications. *Front. Chem.* 2020. V. 8. ID 392. DOI: 10.3389/fchem.2020.00392.
31. **Kargarzadeh H., Mariano M., Gopakumar D., Ahmad I., Thomas S., Dufresne A., Huang J., Lin N.** Advances in cellulose nanomaterials. *Cellulose.* 2018. V. 25. P. 2151-2189. DOI: 10.1007/s10570-018-1723-5.
32. **Kargarzadeh H., Huang J., Lin N., Ahmad I., Mariano M., Dufresne A., Thomas S., Gałęski A.** Recent Developments in Nanocellulose-based Biodegradable Polymers, Thermoplastic Polymers, and Porous Nanocomposites. *Prog. Polym. Sci.* 2018. V. 87. P. 197-227. DOI: 10.1016/j.progpolymsci.2018.07.008.
33. **Klemm D., Cranston E.D., Fischer D., Gama M., Kedzior S.A., Kralisch D., Kramer F., Kondo T., Lindström T., Nietzsche S., Petzold-Welcke K., Rauchfuß F.** Nanocellulose as a natural source for groundbreaking applications in materials science: Today's state. *Mater. Today.* 2018.V. 21. N 7. P. 720-748. DOI: 10.1016/j.mattod.2018.02.001.
34. **Bondeson D., Mathew A., Oksman K.** Optimization of the isolation of nanocrystals from microcrystalline cellulose by acid hydrolysis. *Cellulose.* 2006. V. 13. P. 171–180. DOI: 10.1007/s10570-006-9061-4.
35. **Jiang F., Hsieh Y.-L.** Chemically and mechanically isolated nanocellulose and their self-assembled structures. *Carbohydr. Polym.* 2013. V. 95. N 1. P. 32– 40. DOI: 10.1016/j.carbpol.2013.02.022.
36. **French A.D.** Idealized powder diffraction patterns for cellulose polymorphs. *Cellulose*. 2014. V. 21. P. 885-896. DOI: 10.1007/s10570-013-0030-4.
37. **Jawaid M., Boufi S., Abdul Khalil H.P.S.** Cellulose-Reinforced Nanofibre Composites. Toronto: Woodhead Publ. 2017. 548 p.
38. **Gan P.G., Sam S.T., bin Abdullah M.F., Omar M.F.** Thermal properties of nanocellulose-reinforced composites: A review. *J. Appl. Polym. Sci.* 2020. V. 137. N 11. ID 48544. DOI: 10.1002/app.48544.
39. **Surov O.V., Voronova M.I., Rubleva N.V., Afineevskii A.V., Zakharov A.G.** Cellulose nanocrystals as a compatibilizer for improved miscibility of water-soluble polymer binary blends. *J. Appl. Polym. Sci.* 2019. V. 137. N 19. ID 48662. DOI: 10.1002/app.48662.
40. **Volynskii A.L., Yarysheva A.Y., Rukhlya E.G., Yarysheva L.M., Bakeev N.F.** Specific features of structure and properties of solutions, melts and solid states of polymers in confined nanometric volumes. *Russ. Chem. Rev.* 2014. V. 83. N 11. P. 1003–1026. DOI: 10.1070/RCR4428.

Поступила в редакцию 02.02.2022
Принята к опубликованию 06.07.2022

Received 02.02.2022
Accepted 06.07.2022